EA303 WIND TUNNEL
EXPERIMENT III

AERODYNAMIC CHARACTERISTICS OF AIRFOILS

I. Purpose

1. to reinforce laboratory and wind tunnel operations procedures;
2. to introduce methods of aerodynamic force and moment measurements and reduction of data to standard form;
3. to introduce standard methods of presentation of aerodynamic data.

II. References

1. Rae, W.H., Jr., and Pope, A., *Low Speed Wind Tunnel Testing*, New York: John Wiley & Sons, 1984, 5.1 – 5.6.
2. Anderson, J.D., *Introduction to Flight*, McGraw-Hill, 1989, pp. 178–199.
3. Abbott, I.H., and Von Doenhoff, A.E., *Theory of Wing Sections*, Dover Publications, Inc., 1959, 1.1 – 1.3, 5.1, 5.2, 6.1 – 6.10, 7.1 – 7.6.

III. Introduction

The performance of a wing in subsonic flow depends in large part on the shape of its cross section and the orientation of the cross section to the local resultant flow. A typical section has a rounded leading edge, with smooth upper and lower surfaces having large radii of curvature and coming together to form a sharp trailing edge. Aerodynamic theory tells us this sharp trailing edge is necessary for the generation of lift. The rounded leading edge prevents separation at the leading edge. Consequently, the flow remains attached over the upper surface.

The geometric characteristics that define an airfoil consist of

the chord which is the distance from the leading edge to the trailing edge;

the camber which is the amount of curvature applied to the entire airfoil;

the thickness which is the physical thickness of the section.

The camber line is approximated by simply computing the mean line of the airfoil. The mean line is simply a curve formed from the average ordinates computed along the chord line, i.e.,

$$y_{ml}(x) = \frac{y_u(x) + y_l(x)}{2} \tag{1}$$

A sketch of an airfoil showing its components is given in Fig. 3–1.

The angle of attack is the angle of the section to its resultant flow. For aerodynamic performance this angle is measured relative to the section's orientation when it produces no lift, i.e., its zero lift condition (see Fig. 3–1). For physical reference, the angle of attack is normally measured relative to the geometric chord line. Starting with the geometric chord line at zero angle of attack to the flow, the angle through

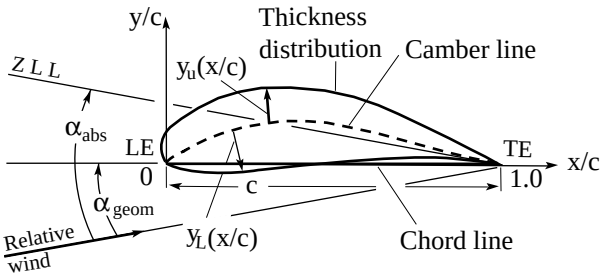

Figure 3–1. Airfoil components.

which the section must be rotated to produce zero lift is the angle of zero lift. The geometric chord angle that produces zero lift is the zero lift line. Interestingly and conveniently the angle of zero lift is constant for a given airfoil section and is determined solely by the camber of the airfoil. Usually an airfoil section with a positive camber had a negative angle of zero lift.

The remote wind, or resultant flow, to which a wing section responds is normally determined by the infinite wind (the flight speed or wind tunnel speed), the wing vortex wake and any disturbances due to fuselage, landing gear, wind tunnel supports, etc. However, when sections are evaluated for aerodynamic performance, it is common to construct an infinite (in span) wing by simply spanning the tunnel from wall to wall with a constant chord wing. This results in an essentially two-dimensional flow, with the flow in each plane perpendicular to the span being equal. The resultant wind, then, is simply the tunnel speed, because effects due to the vortex wake or interference are not present. Another method is to test a rectangular, untwisted, constant cross-sectional wing and correct the data to the infinite wing case.

Historically, several airfoil families were created. The Royal Aircraft Establishment (RAE) generated a large family in the early 1900s. The National Advisory Committee on Aeronautics (NACA) created perhaps the best known families starting in the 1930s. These airfoil sections were created with camber lines determined mathematically. Airfoils were also designed to support specific chordwise load distributions. The thickness distributions are determined mathematically. The airfoil is formed by adding the thickness distribution perpendicular to the camber line. Examples of these families can be found in Ref. 3. Other airfoils include various transonic sections, low Reynolds number sections devised for race cars and sailplanes and sections developed for low drag by maintaining laminar flow over a large portion of the surface. These special airfoil sections and not readily put into families.

IV. Theory

Airfoil theory shows that aerodynamic forces and moments can be expressed in terms of the free stream dynamic pressure, a characteristic length of the model (such as chord) and a dimensionless coefficient that is itself a function of angle of attack, camber, Reynolds number and Mach number. For lift, drag and pitching moment

these become, respectively

$$\frac{L}{b} = \left(\frac{1}{2}\right)\rho V^2 c C_l \tag{2}$$

$$\frac{D}{b} = \left(\frac{1}{2}\right)\rho V^2 c C_d \tag{3}$$

$$\frac{M}{b} = \left(\frac{1}{2}\right)\rho V^2 c^2 C_m \tag{4}$$

where

$$C_l = C_l(\alpha, camber, \mathrm{Re}, \mathrm{M}) \tag{5}$$

$$C_d = C_d(\alpha, camber, \mathrm{Re}, \mathrm{M}) \tag{6}$$

$$C_m = C_m(\alpha, camber, \mathrm{Re}, \mathrm{M}) \tag{7}$$

Note the dimensions of the equations are force and moment *per unit length of span.* This is standard for two-dimensional flow. Another interpretation is to consider 'c' in the equations to be the planform area of a strip of wing 'c' long times unit depth parallel to the span. In this case, the forces and moment have the corresponding units.

In the functional relationships of Eqs. (5, 6, 7), α is the angle of attack of the chord line, Re is the Reynolds number and is interpreted as the ratio of fluid inertial stresses to viscous stresses, and M is the Mach Number, interpreted as the ratio of inertial forces to elastic forces. Mach number measures compressibility effects. For low subsonic flow, $\mathrm{M} \approx 0$ and compressibility effects are unimportant.

The effects of angle of attack and camber are well known. Aerodynamic theory shows, and results are borne out by experiment, that lift and moment are little affected by viscous effects below stall and thus are nearly independent of Reynolds number, Re. Consequently the theory used to predict lift and moment effects at angles of attack below stall is that for an inviscid, incompressible flow in which the only stress is the hydrostatic pressure which amounts to assuming an infinite Reynolds number. This pressure, related to the velocity by the well-known Bernoulli equation, gives the section lift and moment.

Drag, on the other hand, requires consideration of viscous effects and therefore even for angles of attack below stall is dependent on Reynolds number. Summarizing, lift is affected by angle of attack and camber, only camber affects the moment about the aerodynamic center (the aerodynamic center is the location about which the moment is independent of angle of attack), and drag is affected by angle of attack, camber and thickness.

Effects on lift

Theory predicts and experiment verifies that the relationship between C_l and α is essentially linear below stall. Viscous effects have a secondary influence; as Re increases the lift curve slope increases slightly, while if Re decreases the lift curve slope decreases significantly if Re drops below approximately 500,000. Theory predicts a lift curve slope C_{l_α}, i.e., $dC_l/d\alpha$, called a_0, of 2π/radian, while experiment yields roughly 5.73/radian = 0.1/degree.

Stall which is dependent on viscous effects and therefore dependent on Re, for most airfoils, occurs between approximately 12 and 16 degrees angle of attack. Stall occurs at the point at which the upper surface boundary layer has significantly separated resulting in a reduction of the upper surface suction and hence a decrease in the lift. This condition defines $C_{l\,\max}$, the maximum lift coefficient. Operation much beyond stall is not generally useful. Experiment shows that $C_{l\,\max}$ increases with increasing Re. Both $C_{l\,\max}$ and α at which $C_{l\,\max}$ occurs are significantly reduced at Reynolds numbers less than about 500,000. Thin, high speed sections also exhibit reductions, principally due to premature boundary layer separation near the leading edge.

Camber effects are generally limited to effects on the angle of zero lift. This is the angle through which the chord line must be rotated to produce zero lift. (Remember, zero lift is the reference level for aerodynamic performance.) It is usually a negative angle, seldom less than about -4 degrees. Positive camber produces a negative angle of zero lift. Camber is generally less than about 6% of the chord. Positive camber results in a shift in the lift curve to the left. Consequently the angle of attack referenced to the chord line is reduced. Camber also increases $C_{l\,\max}$, but the angle at which $C_{l\,\max}$ occurs may be reduced. This can be seen in Fig. 3–2

Effects on moment

Camber also determines the pitching moment coefficient about the aerodynamic center, $C_{m_{ac}}$. The greater the camber, the more negative the angle of zero lift and the more negative the moment coefficient about the aerodynamic center. Neither of these quantities is significantly dependent on the Reynolds number for Reynolds numbers above 500,000.

Simple inviscid airfoil theory shows that the aerodynamic center is located at the quarter chord, $c/4$. Because of boundary layer and thickness effects, the aerodynamic center may lie between $.21c$ and $.28c$ and be slightly off the chord line. However, $c/4$ is a good easy-to-find reference point. Furthermore, the variation of C_m about $c/4$ with α is linear with a small slope below stall.

In equation form, these results appear as

$$C_l = a_0(\alpha - \alpha_{0L}) \tag{8}$$

$$a.c. = \frac{1}{4}c \tag{9}$$

$$C_{m_{ac}} = \text{function of camber} \tag{10}$$

Here, a_0 is the section lift curve slope with a theoretical value of 2π/radian or, more practically, 0.1/degree. Also notice the linear relation between C_l and angle of attack. Figure 3–2 shows a comparison of lift characteristics between a symmetrical and a cambered airfoil of the same thickness to chord ratio. The lift curve slope, angle of zero lift, maximum lift coefficient and Reynolds number effects are also shown. Figure 3–3 shows a comparison of moment characteristics of a symmetrical and a cambered airfoil of the same thickness to chord ratio. Recall that a symmetrical airfoil has zero camber.

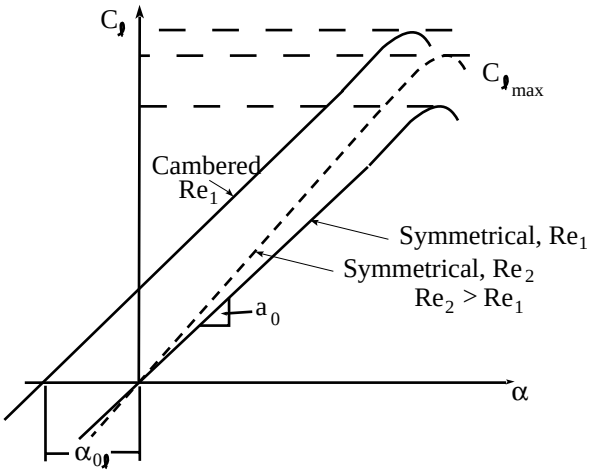

Figure 3–2. Effect of camber and Reynolds number on airfoil lift characteristics.

Effects on drag

The drag coefficient is heavily dependent on viscous effects and thus on the pressure distribution on the airfoil. Hence, it depends heavily on the Reynolds number. Section drag is about equally dependent on skin friction and the pressure distribution. Skin friction drag is due to the viscous shear stress created by the boundary layer on the airfoil surface. It is affected by the viscosity of the fluid, the roughness of the surface, whether the boundary layer is laminar or turbulent, etc. Pressure drag is a result of the fore and aft difference in the pressure distribution on the airfoil. Skin friction drag results from the momentum loss in the boundary layer. At low angles of attack skin friction drag dominates, while at high angles of attack boundary layer separation beginning at the trailing edge and moving forward causes the pressure drag to dominate. At stall and beyond, when the boundary layer has fully separated, the drag is virtually all pressure drag.

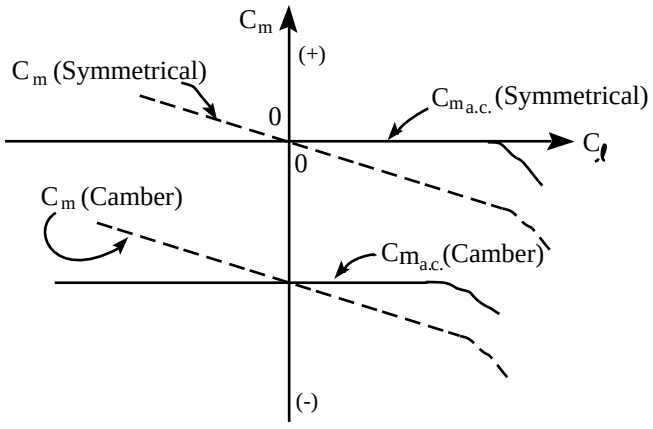

Figure 3–3. Effect of camber on airfoil moment characteristics.

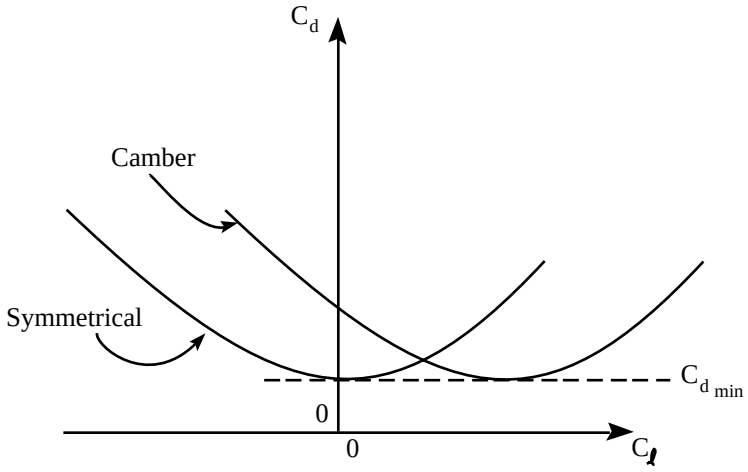

Figure 3–4. Effect of camber on airfoil drag coefficient.

Camber effects on drag coefficient are most significant at the lower angles of attack (or lift coefficients). The effect of positive camber is generally a shift in the minimum drag coefficient, $C_{d\,\min}$, to a positive angle of attack, α. The drag coefficient has a roughly parabolic variation with lift coefficient centered around C_{dmin}. Figure 3–4 shows a comparison of drag characteristics of a symmetrical and a cambered airfoil of the same thickness to chord ratio. This graph of C_d against C_l is referred to as the drag polar.

V. Test Procedure

This test is designed for the pyramidal balance. Two wings of constant 9 in chord that span the tunnel width to within $^1/_{16}$ in of the walls are used. One wing has a constant NACA 0012 symmetrical section and the other a constant NACA 4412 cambered section. Although there is some small remaining tip flow the wings adequately represent an infinite aspect ratio airfoil. Measuring the lift and drag using the pyramidal balance allows direct determination of the profile drag without the use of a wake rake. Tare drag is minimized by use of a movable shroud on the tail pivot arm.

1. Measure ambient pressure and temperature for density, viscosity and Reynolds number calculations.
2. Measure the dimensions of the NACA 0012 wing.
3. Calculate planform area of the wing.
4. Mount the wing in the USNA 44×31 in Eiffel tunnel.
5. Set the tunnel speed to 6 in of alcohol.
6. Sweep through an angle of attack range from -6 degrees to stall in 2 degree increments. Near stall, decrease this to one degree increments. Do not exceed 18 degrees angle of attack.
7. Record angle of attack, lift, drag and pitching moment.
8. At the end of the run, retake ambient pressure and temperature readings.

VI. Data reduction

1. Reduce the data to coefficient form.
2. Graph C_l against α, C_d against C_l and $C_{m_{c/4}}$ against C_l.
3. Determine α_{0l} and $C_{m_{c/4}}$ at ($C_l = 0$). Because the wing is untwisted and of constant section these correspond directly to the section α_{0l} and $C_{m_{ac}}$.
4. Determine the slope of the C_l vs α curve. This is the lift curve slope, a_0, of the airfoil.

Repeat for the NACA 4412 wing. Compare the results to NACA section data (Ref. 3) and to the experimental NACA 0012 data.